Cell PRESS
Structure
Article

The Structure of a Two-Disulfide Intermediate Assists in Elucidating the Oxidative Folding Pathway of a Cyclic Cystine Knot Protein

Maša Cemazar,[1,2] Ajinkya Joshi,[3] Norelle L. Daly,[1,2] Alan E. Mark,[1,3] and David J. Craik[1,2,*]
[1]Institute for Molecular Bioscience
[2]Australian Research Council Special Research Centre for Functional and Applied Genomics
[3]School of Molecular and Microbial Sciences
University of Queensland, Brisbane, QLD 4072, Australia
*Correspondence: d.craik@imb.uq.edu.au
DOI 10.1016/j.str.2008.02.023

SUMMARY

We have determined the three-dimensional structure of a two-disulfide intermediate (Cys^{8}-Cys^{20}, Cys^{14}-Cys^{26}) on the oxidative folding pathway of the cyclotide MCoTI-II. Cyclotides have a range of bioactivities and, because of their exceptional stability, have been proposed as potential molecular scaffolds for drug design applications. The three-dimensional structure of the stable two-disulfide intermediate shows for the most part identical secondary and tertiary structure to the native state. The only exception is a flexible loop, which is collapsed onto the protein core in the native state, whereas in the intermediate it is more loosely associated with the remainder of the protein. The results suggest that the native fold of the peptide does not represent the free energy minimum in the absence of the Cys^{1}-Cys^{18} disulfide bridge and that although there is not a large energy barrier, the peptide must transiently adopt an energetically unfavorable state before the final disulfide can form.

INTRODUCTION

Protein folding remains a major unsolved challenge in modern structural biology. One approach to enhance knowledge about this process is to study the structural characteristics of folding intermediates, transient species that represent specific landmarks along the pathway(s) toward the formation of the native protein state. As well as being important from a fundamental perspective, a greater understanding of these transient structures provides an opportunity to devise therapeutic approaches to diseases originating from protein misfolding and potentially also to help in the development of more efficient methods for the production of recombinant or synthetic proteins for biotechnological applications.

Oxidative protein folding combines the formation of the native global fold of a protein with the oxidation of cysteine residues to form disulfide bridges that stabilize that structure (Cemazar et al., 2004; Wedemeyer et al., 2000). During oxidative folding, partially disulfide-bonded intermediates can in principle be isolated as stable covalent species, facilitating an understanding of the sequence of events that leads to the formation of native disulfide bonds in a given three-dimensional structure. There have been a number of studies of oxidative folding that have characterized the process in terms of the number and types (native versus nonnative) of disulfide bonds present in the intermediates, but few that have studied the actual three-dimensional structure of specific intermediate species. This gap in knowledge reflects the difficulty of structurally characterizing transient species, which may be present only in low concentrations at any moment in time. Oxidative folding studies have been carried out for several different classes of disulfide-rich proteins. Especially well known are the model studies on bovine pancreatic trypsin inhibitor (Creighton, 1974; Weissman and Kim, 1991) and bovine pancreatic ribonuclease A (Scheraga et al., 2001; Wedemeyer et al., 2000). These and other studies have highlighted the fact that there are many different types of oxidative folding mechanisms. However, it is still not clear how a particular amino acid sequence or a particular three-dimensional fold relates to a given mechanism of oxidative folding.

Structural studies of oxidative folding intermediates have been performed mainly using NMR spectroscopy. The proteins studied have typically been small and therefore amenable to solution-state NMR, but the structures of a few folding intermediates have been studied using X-ray crystallography. Most structural studies have been performed using analogs of partially oxidized intermediates containing one or more native disulfide bonds, with the cysteines of the missing disulfide bridge(s) mutated to alanines. These include studies on bovine pancreatic trypsin inhibitor (Staley and Kim, 1992), bovine RNase A (Laity et al., 1997; Pearson et al., 1998; Shimotakahara et al., 1997), leech carboxypeptidase inhibitor (Arolas et al., 2005a), and azurin (Bonander et al., 2000). In general, these studies found that the intermediate analogs were structurally similar to the native structure. Where structural differences were observed, they were restricted to the immediate vicinity of the mutations. Other studies have delineated native-like structures of intermediates that were isolated directly from oxidative folding mixtures. Examples include an intermediate of hen egg white lysozyme (van den Berg et al., 1999) and a three-disulfide isomer of insulin-like growth factor 1 that incorporated one native disulfide bond (Miller et al., 1993). Recently, the notion that native-like structure in intermediate

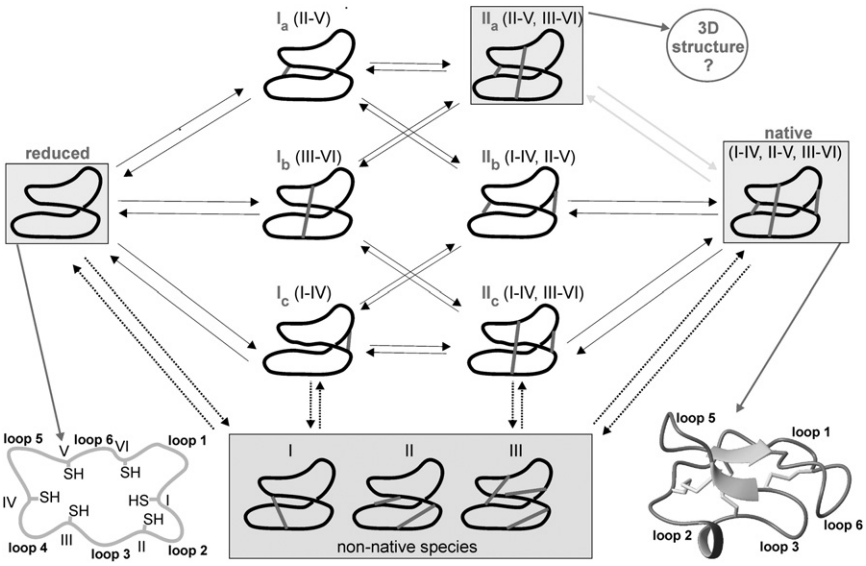

Figure 1. Oxidative Folding Pathways in a Cyclic Cystine Knot Motif

The formation of native disulfide bridges and three-dimensional structure is coupled in the process of oxidative folding. Shown is a schematic representation of the possible folding pathways for the cyclotide MCoTI-II involving intermediate species with native disulfide bonds (center of figure) and others involving nonnative disulfide bonds (box at the bottom). The three important species in the process of oxidative folding are the reduced species, the intermediate II_a, and the native species (highlighted in boxes). The reduced peptide with six reduced cysteine residues (left) oxidizes into one-disulfide intermediate species and subsequently into two-disulfide species, from which a major isomer is observed. This intermediate species, II_a, with two native disulfide bridges converts directly into the native species (light gray arrows). The three-dimensional structural features of the native protein are shown in a ribbon representation at the bottom right. The aim of this work is to determine the three-dimensional structure of the major folding intermediate species, II_a, emphasized by the question mark in the top right corner.

species is favored was reinforced by the determination of the three-dimensional structure of an intermediate of leech carboxypeptidase inhibitor (Arolas et al., 2005b).

One group of disulfide-rich proteins that is of particular interest from a folding perspective is those in which the disulfide bonds interlock to form cystine knots (Craik et al., 2001; Pallaghy et al., 1994). A cystine knot is a structural motif in which two disulfide bonds and their connecting backbone segments form a ring that is threaded by a third disulfide bond. In the case of the cystine knots found in growth factors, the ring involves Cys^{II-V} and Cys^{III-VI} and this is threaded by Cys^{I-IV}, whereas in the inhibitor cystine knot subfamily the ring is formed by Cys^{I-IV} and Cys^{II-V} and is threaded by Cys^{III-VI} (Craik et al., 2001). Given the topological complexity of the cystine knot motif, the questions of how it is formed and what intermediates are present in the oxidative folding pathways are of great interest. Several NMR studies of the formation of cystine knots have provided important insights into the structures of such intermediates. These include the structural characterization of a three-disulfide intermediate from *Amaranthus* α-amylase inhibitor containing three nonnative disulfides (Cemazar et al., 2003, 2004) and an alkylated version of an intermediate from *Ecballium elaterium* trypsin inhibitor II with two native disulfides and a native-like structure (Le-Nguyen et al., 1993).

In the current study, we report the three-dimensional structure of a two-disulfide folding intermediate of the cyclic cystine knot protein MCoTI-II (*Momordica cochinchinensis* trypsin inhibitor II), categorized both as a cyclic knottin (Chiche et al., 2004) and a member of the cyclotide family of plant defense proteins (Craik, 2006; Craik et al., 2006a, 2006b). Cyclotides have a cyclic peptide backbone as well as a cystine knot, and the combination of these two structural features makes them extremely stable toward thermal, enzymatic, and chemical challenges (Colgrave and Craik, 2004; Craik et al., 1999). Cyclotides are also functionally diverse and display bioactivities ranging from antimicrobial activity, enzyme inhibitory action, and anti-HIV activity to insecticidal properties, making them attractive candidates for both drug design and agricultural applications (Craik, 2006; Craik et al., 2004, 2006b; Goransson et al., 2004; Gustafson et al., 2004).

An understanding of the molecular basis of the oxidative folding of cyclotides could potentially assist in the design of engineered cyclotide analogs with novel bioactivities. The three-dimensional structure of a double alanine mutant corresponding to a two-disulfide intermediate of the prototypic cyclotide kalata B1 was reported recently (Daly et al., 2003). Interestingly, this major native-like two-disulfide intermediate does not lead directly to the native structure and requires disulfide shuffling for eventual formation of the cystine knot (Craik and Daly, 2005; Daly et al., 2003). The oxidative folding pathway of MCoTI-II was elucidated recently and, like kalata B1, is characterized by the accumulation of a native two-disulfide species lacking the I-IV disulfide bond (Cys^1-Cys^{18}). However, in contrast to the kalata B1 intermediate, the MCoTI-II intermediate is a direct precursor of the native protein (Cemazar et al., 2006). Figure 1 shows the three-dimensional structure of MCoTI-II and defines the naming of the intracysteine loops on its cyclic scaffold. These loops project from the cystine knot core and are the locations of exposed residues responsible for activity in cyclotides. A schematic illustration of the oxidative folding pathway for MCoTI-II is also shown in Figure 1, including a representation of the fully reduced species, some partially oxidized species, and the two-disulfide intermediate referred to as II_a that is the subject of the current study. Partially oxidized intermediates have been observed in a number of other cystine knot proteins, other three- and four-disulfide proteins, and also for the trypsin inhibitor EETI-II, which shares high sequence and structural similarity with MCoTI-II (Heitz et al., 1995; Le-Nguyen et al., 1993).

The crucial questions that this study aimed to address are whether the native fold represents a minimum in the energy landscape of the peptide in the absence of the disulfide bridges and,

if the disulfide bridges are required for the peptide to adopt the native fold, at what stage along the folding pathway does the structure become native like? To answer these questions, we determined the three-dimensional structure of a key two-disulfide intermediate of MCoTI-II using NMR spectroscopy. Furthermore, molecular dynamics simulations were used to gain insight into the conformational changes that occur as the last native disulfide is formed. To our knowledge, the derived structure is one of only two cases in the literature where the full three-dimensional structure of an intermediate directly isolated from a folding pathway has been determined. The results show that the native fold is energetically less favored than the intermediate fold but the native MCoTI-II structure is facilitated by the formation of the I-IV disulfide bridge, which locks the protein into the native fold.

RESULTS

The main aim of this work was to determine the three-dimensional structure of the major two-disulfide intermediate that accumulates during the oxidative folding of MCoTI-II. Native MCoTI-II was extracted from the seeds of *M. cochinchinensis*, purified, and reduced to remove the disulfide bonds. The intermediate was prepared in sufficient quantity for NMR structural characterization by isolating it from an oxidative refolding reaction starting from the reduced peptide (Cemazar et al., 2006; Hernandez et al., 2000). The most important issue when studying solution structures of transient oxidative folding species with NMR is their stability. The stability of II_a was determined under the conditions used for the NMR experiments and the half-life of conversion to the native state was ~100 hr, more than sufficient for two-dimensional NMR analysis. After recording a 16 hr two-dimensional NMR spectrum, less than 5% of II_a had converted to the native conformation. Nevertheless, the peptide was purified prior to recording each series of two-dimensional NMR spectra and never kept in solution for more than 24 hr. The conditions used for recording spectra necessarily included 0.1% TFA to slow the oxidation of the two reduced thiol groups to a third disulfide. This meant that the structure of the intermediate was determined at pH 2, but in any case was expected to be similar at more neutral pH based on a lack of change in backbone chemical shifts of the parent peptide with pH (Table S1, see the Supplemental Data available with this article online).

Three-Dimensional Structure of the Two-Disulfide Intermediate II_a

Two-dimensional NMR spectra of II_a recorded at 600 MHz were of high quality with excellent signal dispersion, indicative of a well-structured peptide. No extra spin systems that might indicate conformational heterogeneity were observed. Full assignments of the backbone and side-chain resonances were achieved using ^{1}H two-dimensional sequential assignment strategies. II_a contains two reduced cysteines, Cys^1 and Cys^{18}, which normally form the I-IV disulfide of the cystine knot in the native peptide. Because it was previously shown (Cemazar et al., 2006) that the chemical shifts of the backbone H_α protons of II_a are similar to those of the native protein, it was concluded that the two disulfide bonds of II_a are the two remaining native disulfides of the cystine knot, that is, Cys^8-Cys^{20} and Cys^{14}-Cys^{26}.

Table 1. Structural Statistics for Intermediate II_a

II_a (Disulfides: 8–20, 14–26)	
Pairwise Rmsd (Å)	
Mean global backbone (1–34)	2.13 ± 0.59
Mean global heavy chain (1–34)	2.82 ± 0.58
Mean global backbone (6–26)	0.47 ± 0.17
Experimental Data	
Distance restraints	147
Long-range	28
Medium-range	26
Sequential	93
Dihedral restraints	22
H-bonding restraints	8
NOE violations > 0.3 Å	0
Dihedral violations > 3.5°	0

The initial structural calculations were performed with the inclusion of these two disulfide links, but this connectivity pattern was subsequently confirmed using two independent strategies (see below).

The three-dimensional structure of II_a was calculated by simulated annealing in the presence of distance restraints based on NOE crosspeak intensities, backbone and side-chain dihedral angle restraints derived from coupling constants and NOE patterns, and hydrogen-bonding restraints derived from amide H/D exchange data. The restraints are summarized in Table 1 along with the structural and energetic statistics for the final family of 20 structures. All of the structures are in good agreement with the experimental data and have good covalent geometries, as evident from low deviations from optimal bond lengths and angles, and from the Ramachandran statistics.

It is clear from the structural statistics for II_a that the superposition of the peptide backbone for the family of 20 lowest-energy structures is excellent in the region Lys^6-Cys^{26}, but that there is increased disorder in the region corresponding to loops 1 and 6. An overlay of the 20 lowest-energy structures gives a root-mean-square deviation (rmsd) of 0.47 Å for the backbone in the region Lys^6-Cys^{26}, and 2.13 Å over the whole structure. The disorder in the structural ensemble most likely reflects intrinsic flexibility, but other factors such as a reduced density of structural restraints in the disordered regions cannot be excluded. The flexibility explanation is consistent with the fact that the H_α chemical shifts in loops 1 and 6 are close to random coil values.

An overlay of the 20 lowest-energy structures and a representation of the three-dimensional structure of II_a and native MCoTI-II are shown in Figure 2, from which it is clear that the regions with well-defined secondary structural features (i.e., residues 6–26) are where the intermediate is most similar to the native conformation. Both structures feature two antiparallel β strands (residues 19–20 and 26–27), which combined with a type I β turn (residues 21–24) makes a β hairpin (residues 19–27). A 3_{10} helix located between residues 10 and 14 in loop 3 is also found in both the intermediate and native structures (Felizmenio-Quimio et al., 2001; Heitz et al., 2001). Several β and γ turns are also conserved. However, a marked difference between the structures is that the two reduced cysteine side

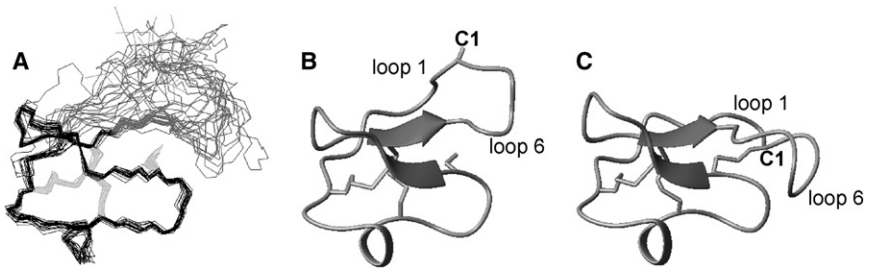

Figure 2. Three-Dimensional Structure of II_a and Comparison with Native MCoTI-II

(A) Superimposition of the peptide backbone of the 20 lowest-energy structures representing the solution structure of intermediate II_a.

(B) Ribbon diagram of II_a with the side chains of the cysteine residues as lines.

(C) Ribbon diagram of native MCoTI-II with the side chains of the cysteine residues as lines in the same orientation as the structure of II_a in (B).

chains (Cys^1 and Cys^{18}) point in opposite directions and their sulfur atoms are separated by up to 12.9 Å in the intermediate structure. This is in contrast to the native conformation, where these sulfur atoms are linked in a disulfide bond with a distance between them of ~2.0 Å.

After the dissolution of II_a in ^2H_2O, several slowly exchanging amide protons were detected after more than 5 hr, including the amides of Cys^8, Ile^{19}, Arg^{21}, Gly^{24}, Tyr^{25}, Cys^{26}, and Gly^{27}, the majority of which are a part of the β hairpin. The large number of amide protons in slow exchange with the solvent reinforces the fact that the intermediate species is well structured.

Three-Dimensional Structures of Alternative Disulfide Isomers

Because of the similarity of the chemical shifts of II_a to the native species, it was hypothesized that the two disulfides present are the native disulfides of the cystine knot, Cys^8-Cys^{20} and Cys^{14}-Cys^{26}. To substantiate this hypothesis, we performed structure calculations with all three possible connectivities of the four disulfide-bonded cysteine residues, that is, the native connectivity, Cys^8-Cys^{20}, Cys^{14}-Cys^{26}, and the two alternative connectivities, Cys^8-Cys^{14}, Cys^{20}-Cys^{26} and Cys^8-Cys^{26}, Cys^{14}-Cys^{20}. A comparison of the statistics for the three calculations is given in Table 2. The three structures all have the same overall fold, featuring a β hairpin in the middle of the structure, a 3_{10} helix turn, and a disordered loop 6, as seen in Figure 3. Consistent with our hypothesis, the native connectivity Cys^8-Cys^{20}, Cys^{14}-Cys^{26} is energetically favored over the other two disulfide connectivities. For example, the NOE energies for the two nonnative forms are ~30 kJ/mol, whereas for the native connectivity the energy is ~10 kJ/mol. Furthermore, from the rmsd values and the statistics from the Ramachandran plot, it is apparent that the existence of the two native disulfide bonds is favored over the other disulfide pairings. It can be concluded from these results that II_a is a partially oxidized species with two native disulfide bonds.

Additional proof for the native disulfide connectivity in the intermediate species was obtained from an analysis of the χ^1 dihedral angles of the cysteine residues. It has been shown previously (Rosengren et al., 2003) that disulfide connectivity of cyclotides can be uniquely discriminated by the combined side-chain conformations of the three disulfide bonds. Typically,

Table 2. Energies and Geometric Statistics for the Three Possible Disulfide Connectivities of Two-Disulfide Intermediates

	8–20, 14–26	8–26, 14–20	8–14, 20–26
Energies (kJ/mol)			
Overall	−1045.8 ± 30.0	−893.5 ± 29.6	−944.3 ± 17.3
Bonds	6.1 ± 0.6	13.8 ± 1.1	10.9 ± 1.4
Angles	36.8 ± 4.7	72.9 ± 5.1	56.8 ± 6.8
Improper	5.7 ± 1.3	12.6 ± 1.5	11.1 ± 1.8
van der Waals	−61.1 ± 10.0	−37.4 ± 9.5	−32.3 ± 11.8
NOE	10.4 ± 2.6	35.4 ± 4.5	31.6 ± 10.7
Experimental dihedral angles	0.37 ± 0.2	24.2 ± 2.1	7.5 ± 1.3
Dihedral	148.0 ± 8.9	157.4 ± 9.9	166.7 ± 16.7
Electrostatic	−1192.0 ± 36.8	−1172.4 ± 35.0	−1196.9 ± 25.6
Rmsd			
Bonds (Å)	0.0036 ± 0.0002	0.0054 ± 0.0002	0.0048 ± 0.0003
Angles (°)	0.532 ± 0.033	0.750 ± 0.026	0.661 ± 0.040
Improper (°)	0.397 ± 0.045	0.593 ± 0.035	0.556 ± 0.043
NOE	0.037 ± 0.005	0.070 ± 0.004	0.065 ± 0.010
Experimental dihedral angles	0.50 ± 0.20	4.34 ± 0.19	2.41 ± 0.21
Ramachandran (residues 6–26) (%)			
Most favored	85.0	67.1	71.2
Additionally allowed	15.0	31.2	27.6
Generously allowed	0	1.8	1.2
Disallowed	0	0	0

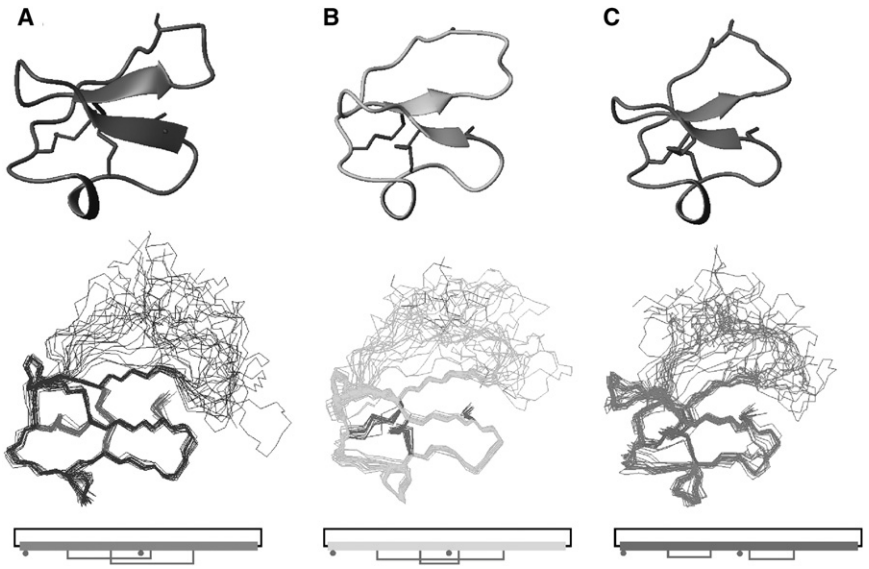

Figure 3. Three-Dimensional Structures of Possible Intermediates with Alternative Disulfide Pairings

The ribbon representation (top), the overlay of 20 minimum-energy structures (middle), and the disulfide connectivity patterns of possible isomers of II_a (bottom).

(A) Cys^8-Cys^{20}, Cys^{14}-Cys^{26}.

(B) Cys^8-Cys^{26}, Cys^{14}-Cys^{20}.

(C) Cys^8-Cys^{14}, Cys^{20}-Cys^{26}.

χ^1 angles can be placed into one of the three staggered conformations (−60°, +60°, or 180°, with an uncertainty of ±30°) by combining the information from $^3J_{H\alpha H\beta}$ coupling constants with the interproton HN-Hβ distances (Lovelace et al., 2006; Rosengren et al., 2003). The former were extracted from ECOSY spectra, whereas the latter were derived from short mixing-time NOESY spectra. For cysteines 18 and 26, patterns of one large and one small $^3J_{H\alpha H\beta}$, together with one strong and one weak HN-Hβ NOE, are observed, consistent with dihedral angles of −60° ± 30°, and cysteines 14 and 20 display one large and one small $^3J_{H\alpha H\beta}$ combined with two strong HN-Hβ NOEs, consistent with χ^1 dihedral angles of 180° ± 30°. A comparison of these experimental χ^1 dihedral angles to the values in the calculated structures unequivocally shows that the combination was consistent only with the II-V, III-VI connectivity (see Table 3). In this context, "experimental" χ^1 dihedral angles refer to values deduced directly from local NMR parameters, and not influenced by any computational algorithms.

Molecular Dynamics Simulations

A series of molecular dynamics simulations of partially reduced MCoTI-II peptide without the disulfide bridge I-IV starting from both the native fold (Protein Data Bank [PDB] ID code: 1IB9) and the intermediate structure (reported in this work) was performed. The simulations were designed to investigate whether the native three-dimensional fold of MCoTI-II represents a local minimum in the free energy surface of the partially reduced peptide without the disulfide bond I-IV. The three-disulfide form of MCoTI-II was also simulated as a control starting from the native fold under identical conditions. Figure 4A shows an overlay of time snapshots from the simulation of the fully oxidized form starting from the native fold (thick black line). The overall fold of the fully oxidized species is clearly stable. The average backbone rmsd with respect to the starting structure over the 50 ns of the simulation was 2.0 Å. This deviation was primarily associated with fluctuations within loops 1 and 6 and variations in the region of the 3_{10} helix. Following the reduction of the I-IV disulfide

Table 3. Dihedral Angle Analysis[a] of Alternative Disulfide Isomers of Intermediate II_a

	Native MCoTI-II	II_a			
Residue	PDB ID Code 1ib9[b]	Experimental[c] (±30°)	(8–20, 14–26)	(8–14, 20–26)	(8–26, 14–20)
1	−165	N/A	Disordered	Disordered	Disordered
8	58	N/A	52 ± 7	−14 ± 28	0.2 ± 27
14	−180	−180	−151 ± 4	−139 ± 8[d]	−143 ± 2[d]
18	−83	−60	−54 ± 7	−62 ± 3	−55 ± 6
20	−168	−180	−170 ± 4	−134 ± 1[d]	−144 ± 1[d]
26	−62	−60	−66 ± 11	−55 ± 9	−47 ± 7

N/A, not available.

[a] The data show a comparison between experimentally deduced χ^1 angles (in degrees) based on local NMR data for cysteine residues in II_a and the calculated angles in simulated annealing structures with the three possible disulfide connectivities. The data confirm that the disulfide connectivity in the intermediate is native like (8–20, 14–26), as the calculated angles deviate from the experimental ones by more than ± 30° for at least two Cys residues in each of the alternative disulfide connectivities.

[b] Literature data for MCoTI-II are included for comparison.

[c] Deduced from raw NMR data including $J_{\alpha\beta}$ coupling constants and intraresidue NOE intensities (Rosengren et al., 2003).

[d] These χ^1 angles violate in the structure calculations by more than ±30° as a result of the restraints imposed by the disulfide connectivity.

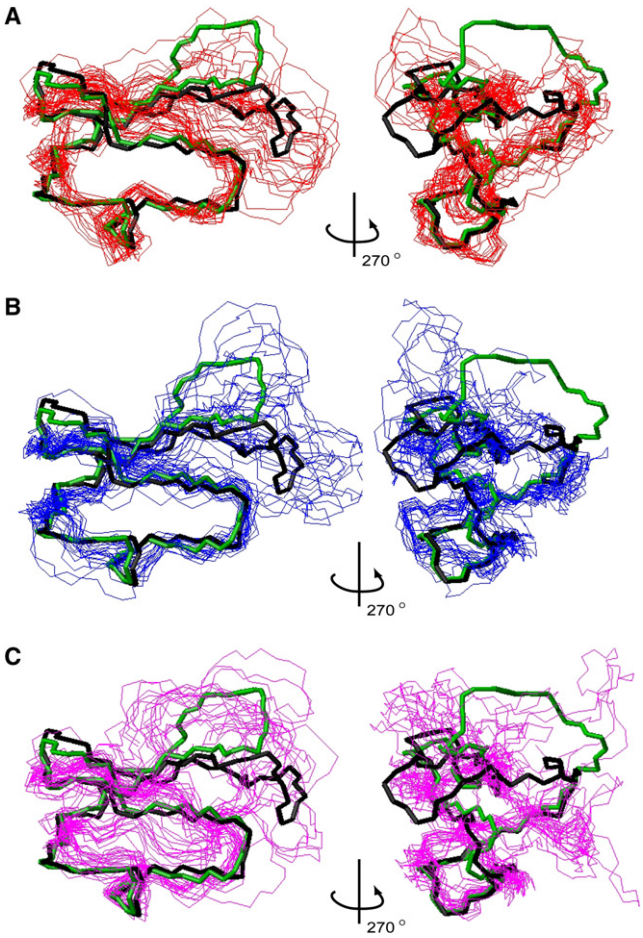

Figure 4. Molecular Dynamics Simulations of the Intermediate and the Native State

An overlay of the NMR structures of the native MCoTI-II (black thick line), the intermediate II_a (green thick line), and structures obtained from molecular dynamics simulations.

(A) Twenty structures taken at 2.5 ns intervals from the MD simulations starting from the NMR structure of the native MCoTI-II (PDB ID code: 1IB9) with three disulfides.

(B) Twenty structures taken at 2.5 ns intervals from the MD simulations starting from the NMR structure of the native MCoTI-II (PDB ID code: 1IB9) with a reduced Cys^1-Cys^{18} disulfide bond.

(C) Twenty structures taken at 2.5 ns intervals from the MD simulations starting from the NMR structure of the folding intermediate II_a (with two disulfide bonds, II-V and III-VI).

bridge, dramatic changes in the conformation of loops 1 and 6 were observed. Figure 4B shows an overlay of structures sampled every 2 ns for the two-disulfide species. A backbone least-squares fit of the structures was performed using residues 6–26 to highlight motion within loops 1 and 6. It is clear that these loops, comprising residues 27–34 and 1–5, sample a wide range of alternative conformations but do not converge to the proposed NMR structure of the intermediate (thick green line). The average rmsd over the 50 ns of the simulation was 3.2 Å with respect to the native structure and 6.0 Å with respect to the NMR structure of the intermediate. Figure 4C shows an overlay of snapshots from a simulation of the two-disulfide form starting from the NMR structure of the intermediate proposed in this work. Again, loops 1 and 6 are highly mobile and sample a range of conformations. Although the structure moves away from that of the intermediate, the conformations sampled do not correspond to those sampled in the simulation starting from the native fold. This suggests that 50 ns is too short to have sampled all of the accessible conformational space. The average rmsd over the 50 ns of the simulation starting from the intermediate was 3.4 Å with respect to the native fold and 4.2 Å with respect to the NMR structure of the intermediate. These deviations occur primarily within loops 1 and 6, with the average rmsd of the backbone of residues 6–26 during the simulation with respect to the NMR structure of the intermediate being just 2.0 Å.

DISCUSSION

In this study, we have determined the three-dimensional structure of an oxidative folding intermediate that is observed on the pathway to formation of a topologically complex structural motif known as the cyclic cystine knot. The study elucidates the structural changes that MCoTI-II undergoes in forming the final covalent link, namely the third disulfide bridge, to complete the cyclic cystine knot motif. The findings are potentially of broad interest, as cystine knots are present in a large range of proteins, including growth factors, toxins, and inhibitors (Craik et al., 2001; Pallaghy et al., 1994). This study represents one of only a few structural characterizations of an oxidative folding intermediate species and is important because it provides a snapshot of a key intermediate that is unperturbed by extraneous substitutions normally required to investigate such species. Several structures of serine or alanine double mutants of intermediates have shed light on the structures that could be involved in the oxidative folding of other proteins, but there is always the possibility that the mutations perturb the system and may not provide an accurate picture of the folding process. Recently, the structure of an intermediate directly isolated from the folding reaction was reported for leech carboxypeptidase inhibitor (Arolas et al., 2005a), and the need for more high-resolution structures of "real" intermediates was emphasized (Arolas et al., 2006).

It is important to note that although our approach has the advantage of being nonperturbing from a mutagenesis perspective, it has the potential limitation that structural studies involving partially oxidized intermediates require a low pH to minimize thiol-disulfide exchange. The deduced structures may therefore be different from those at more physiological pH, but we believe that this is not the case for the MCoTI-II intermediate, because cyclic cystine knot peptides are very rigid and we detected no significant change (<0.063 ppm) in the backbone chemical shifts of MCoTI-II as pH was varied. Even though the MCoTI-II intermediate has only two of the three disulfides of the cystine knot motif, it has been shown previously that the rigidity of this intermediate is maintained (Cemazar et al., 2006).

In general, mechanisms of oxidative folding are not yet fully understood, but several attempts have been made at defining the roles of the amino acid sequence and disulfide bonds in this process. Anfinsen's hypothesis that the amino acid sequence solely determines the three-dimensional fold is still the basis for the understanding of protein folding (Anfinsen, 1973). It has been suggested that folding involving the formation of

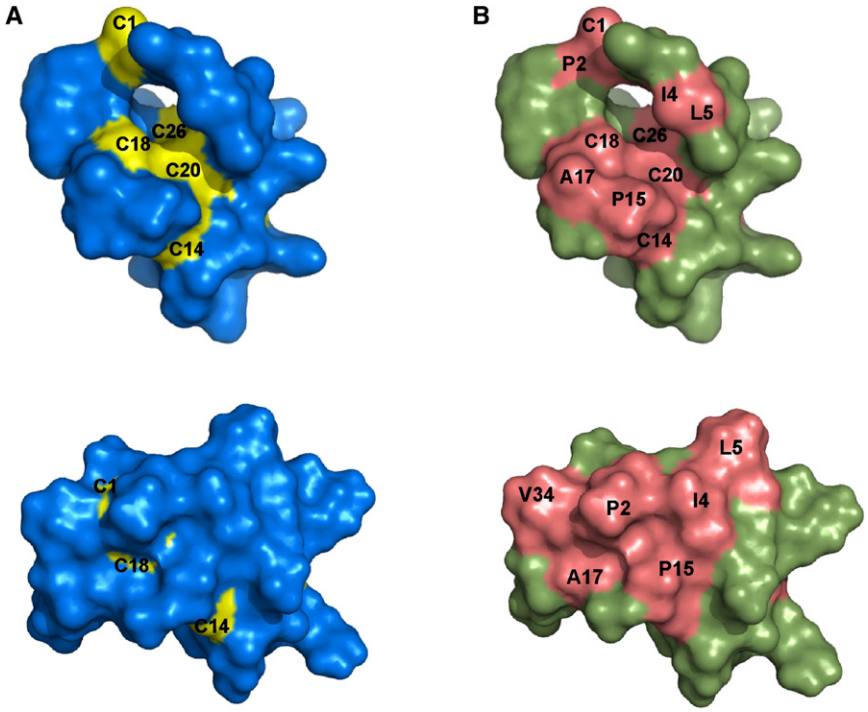

Figure 5. Surface-Exposed Residues

(A) Surface-exposed cysteine residues in intermediate (above) and the native MCoTI-II (below). Cysteines are colored in yellow and noncysteine residues in blue.

(B) Surface-exposed hydrophobic residues and cysteine residues in intermediate (above) and the native MCoTI-II (below). Hydrophobic residues and cysteines are colored in red and hydrophilic residues in green.

disulfide bonds is directed by native-like interactions between segments of secondary structure and that disulfide bonds can promote folding by restricting the search in conformational space by crosslinking the protein in its unfolded state, thus decreasing its entropy (Arolas et al., 2006; Cemazar et al., 2003). The formation of disulfide bonds and thus the existence and stability of oxidative folding intermediates are influenced by the solvent accessibility, and by the reactivity and proximity, of the thiol groups and disulfide bonds. The existence and stability of intermediates provide insight into the mechanism of oxidative protein folding. The mechanisms studied to date have in general been characterized in terms of different heterogeneities of folding intermediates, the predominance of intermediates containing native disulfide bonds, and the presence or absence of intermediates with nonnative disulfide bonds species. Recently, there have been an increasing number of studies that include structural information about intermediate species, thus providing detailed insight into the oxidative folding mechanism.

The present study focuses on determining the structure of a native two-disulfide intermediate species and at defining its role in the oxidative folding of MCoTI-II. The structures of the native and the intermediate appear similar in most regions, with the major differences occurring between Cys^{1}-Ile^{4} and Ala^{17}-Ile^{19}. These coincide with the regions where the two cysteines that eventually make up the missing disulfide bridge (Cys^{1}-Cys^{18}) are located. One interesting feature of the structure of II_a is the disorder in loops 1 and 6, which are also in the regions that differ most between the two species. It has been suggested that in the native protein the array of different conformations for loops 1 and 6 reflects flexibility rather than just a lack of structural restraints (Felizmenio-Quimio et al., 2001). The same is true for the intermediate state as reflected by the random coil-like values of the H_α chemical shifts in these two loops.

The hydrogen-bonding network in the CCK motif of MCoTI-II was determined using H/D exchange experiments on the native and carboxyamidomethylated intermediate species 2CM-II_a (Cemazar et al., 2006). It is clear from these studies that the overall hydrogen-bonding network is not disrupted when the disulfide bond Cys^{1}-Cys^{18} is absent, but there is a general loosening of the scaffold which is apparent from the increased number of backbone amide protons that have faster exchange rates with the solvent. From the present study, it is clear that the number of slowly exchanging amide protons in the intermediate II_a is comparable to the number typically seen for three-disulfide cyclotides such as the native species MCoTI-II, providing another indication that this intermediate is comparable in its rigidity to its three-disulfide counterpart.

It is clear from the difference between the three-dimensional structures of the native and the intermediate state that the position and orientation of loops 1 and 6 have to change before the final disulfide bond can be formed. Two cysteines (Cys^{1} and Cys^{18}) have to come into close proximity to be able to oxidize into the disulfide bridge I-IV. It is interesting to speculate on the main differences in the interactions that stabilize the native and the intermediate states. One contribution to the stability of the native state may be the gain in the solvation energy upon oxidation of the solvent-exposed side chains of the two free cysteine residues. The surface accessibilities of the two cysteines in the intermediate (Cys^{1} and Cys^{18}) are greater than in the native state (Cys^{1}: 35.4% versus 3.8%; Cys^{18}: 5.5% versus 3.5%), suggesting that once these two cysteines have oxidized, particularly one of them gets buried within the protein core. This can be seen on the surface representation in Figure 5A, where the cysteine residues are buried in the native state but are well exposed on the surface in the intermediate. The accessibilities of the other cysteines located in the core of the three-dimensional structure are also smaller in the native conformation.

Another important difference in the way the intermediate and the native state are stabilized relates to interactions between hydrophobic residues. The typical hydrophobic core seen in most globular proteins is replaced in cyclotides by the six cysteines making up the cystine knot motif, which leaves the other hydrophobic residues in a solvent-exposed position. This is also observed for both the native and the intermediate MCoTI-II species. The surface representation of both species in Figure 5B shows

that in the intermediate there are two distinct patches of hydrophobic residues. One is located across the flexible loops 1 and 6 (Val^{34}, Cys^{1}, Pro^{2}, Ile^{4}, Leu^{5}) and the other is in loop 3 (Pro^{15}, Ala^{17}, Cys^{18}). However, in the native state, these two hydrophobic patches collapse together and form a single hydrophobic surface. This can be seen, for example, from the proximity of pairs of hydrophobic residues in the native state that are located farther apart in the intermediate structure, Pro^{15}, Pro^{2} and Ala^{17}, Val^{34}. There is also a marked difference in the surface accessibilities of the hydrophobic residues in loop 3 of the native state relative to the intermediate state (Pro^{15}: 33.9% versus 19.9%; Ala^{17}: 28.9% versus 10.0%). This region corresponds to the point where loop 6 comes into contact with the core of the structure, suggesting that there may be a favorable energy gain upon burial of some of the cysteine residues and upon the joining of the hydrophobic patches. These may be some of the important differences in the interactions that stabilize the intermediate and the native state.

Molecular dynamics simulations of the MCoTI-II peptide without the disulfide I-IV, starting both from the native fold and from the NMR structure of the intermediate, both diverge from their initial starting structures. This suggests that loops 1 and 6 are flexible and able to sample a wide range of conformational space. The fact that the structure does not remain close to the native fold of the fully oxidized species suggests that it is not a local minimum in the free energy surface once the I-IV disulfide is reduced. The NMR structure of the intermediate also does not appear to represent a well-defined conformation in the simulations. In fact, starting from the proposed NMR structure of the intermediate, the conformations sampled during the simulations were on average closer to the native fold than to that of the intermediate (results not shown). Both the NMR and the simulation results suggest that the native fold is stabilized by the free energy of disulfide bridge formation. Experimentally, the disulfide bridge I-IV is thermodynamically less stable than the other disulfide bridges II-V and III-VI: it is the first bridge to be reduced when a reducing agent is present in the solution with fully oxidized MCoTI-II (Cemazar et al., 2006). Before the final disulfide bridge can form, the molecule must adopt the energetically unfavorable native fold. Finally, there is a rate-determining step leading to the formation of the final disulfide bridge, which stabilizes the structure in the native fold.

In conclusion, here we have reported a full three-dimensional structure of a partially oxidized folding intermediate of MCoTI-II. This is a clear example of a case in which the native structure is held together by the formation of a specific disulfide bridge, and the native conformation is not the lowest free energy state in the absence of the disulfide bridge I-IV. The native fold is instead energetically less favored and is held together by the formation of this specific disulfide bridge, which locks the protein into the native fold.

EXPERIMENTAL PROCEDURES

Isolation of MCoTI-II II_a

Native MCoTI-II was extracted from the dormant seeds of *M. cochinchinensis* as described previously and purified using RP-HPLC (Hernandez et al., 2000). On the oxidative folding pathway there are a number of one-disulfide species present, I_a, I_b, and I_c, and two-disulfide species, II_a and II_b, of which II_a is the most abundant. A sample of the intermediate II_a was isolated from the oxidative folding mixture of reduced MCoTI-II after 60 min (0.1 M NH_4OAc [pH 8.5], 2 mM reduced glutathione, 0.1 mg/ml MCoTI-II at 25°C). It has been shown previously that at this time point the two-disulfide intermediate II_a is the most abundant species (Cemazar et al., 2006). The reaction was quenched with 4% trifluoroacetic acid and II_a was purified using a semipreparative RP-HPLC (250 × 10 mm, 4 μm) C18 column with a linear gradient of solvent A (H_2O/0.05% TFA) and B (90% CH_3CN/10% H_2O/0.05% TFA) at a flow rate of 3.0 ml/min. The purity of the sample was confirmed using analytical RP-HPLC and electrospray ionization mass spectrometry and was found to be >98%.

NMR Experiments

Samples of II_a were prepared by dissolving the peptide in 90% H_2O, 10% D_2O, 0.1% TFA to a concentration of ~0.6 mM. The trifluoroacetic acid was used to maintain a pH of 2 to prevent the oxidation and/or reshuffling of cysteine residues. Spectra were recorded on a Bruker ARX 500 or a Bruker ARX 600 NMR spectrometer at 290K. For TOCSY experiments, the mixing time was 80 ms and for NOESY the mixing time was 200 ms. Slowly exchanging amide protons were identified by recording a series of one-dimensional and TOCSY spectra at 290K over 20 hr immediately after dissolution of a sample in 100% D_2O, 0.1% TFA. Two-dimensional spectra were collected with 4096 data points in the f2 dimension and 512 increments in the f1 dimension and processed using Topspin (Bruker) software. The f1 dimension was zero filled to 2048 real data points, with the f1 and f2 dimensions were multiplied by a sine-squared function prior to Fourier transformation.

Structure Calculations

Preliminary structures of II_a were calculated using a torsion angle simulated annealing method within the program DYANA (Guntert et al., 1997). Final structures were calculated by a combination of simulated annealing and energy minimization using CNS version 1.2 (Brünger et al., 1997). The Asp side chains were assumed in the carboxyl protonated state to reflect the experimental conditions (pH 2). The starting structures were generated using random (φ,ϕ) dihedral angles and energy minimized to produce structures with the correct local geometry. A set of 50 structures was generated by a torsion angle simulated annealing method (Rice and Brünger, 1994; Stein et al., 1997). This involved a high-temperature phase comprising 4000 steps of 0.015 ps of torsion angle dynamics, a cooling phase with 4000 steps of 0.015 ps of torsion angle dynamics during which the temperature is lowered to 0K, and finally energy minimization by 500 steps of Powell minimization. Structures consistent with restraints were subjected to further molecular dynamics and energy minimization in a water shell, as described by Linge and Nilges (1999). The refinement in explicit water involved the following steps: first, heating to 500K in intervals of 100K, each comprising 0.25 ps of dynamics in Cartesian space using 5 fs time step, and second, 12.5 ps of dynamics at 500K before a cooling phase where the temperature is lowered in 100K intervals each comprising 12.5 ps of dynamics. Finally, the structures were minimized with 2000 steps of Powell minimization. Three sets of structures were calculated corresponding to the three possible connectivities: (II-V, III-VI), (II-III, V-VI), and (II-VI, III-V), as described in Results. The native connectivity (II-V, III-VI) was the only one consistent with the observed χ_1 angles (Table 3). Structures were analyzed using PROMOTIF (Hutchinson and Thornton, 1996) and PROCHECK-NMR (Laskowski et al., 1996).

Molecular Dynamics Simulations

All simulations were performed using the GROMOS96 package (Scott et al., 1999) in conjunction with GROMOS 53a6 force field (Oostenbrink et al., 2004). Three different systems were simulated for comparison. They were (1) the fully oxidized structure starting from the native conformation, (2) a two-disulfide species without the disulfide Cys^{1}-Cys^{18} starting from the native conformation, and (3) the two-disulfide intermediate Cys^{8}-Cys^{20}, Cys^{14}-Cys^{26} starting from the NMR structure of II_a obtained as described above. The structure of Felizmenio-Quimio et al. (2001) (PDB ID code: 1IB9) was used as the starting conformation for the simulation of systems 1 and 2. Each system was placed in a periodic truncated octahedron box (box edge = 5.5 nm) and solvated with 2614 simple point charge (Berendsen et al., 1981) water molecules. The temperature (300K) and pressure (1 atm) were maintained by weak coupling to an external temperature and pressure bath (Berendsen

et al., 1984) using coupling times of 0.1 and 0.05 ps, respectively. The time step was 2 fs. A twin range cutoff of 0.8 and 1.4 nm was used. A reaction field correction was applied to account for the truncation of electrostatic interactions beyond the long-range cutoff. After minimization, each system simulated for 50 ns. Note that the protonation states of all residues except for Asp12 were set appropriate to pH 2. In the native structure, Asp12 interacts strongly with Arg8 and Arg9. As the native structure was solved at pH 3.5, the protonation state of this residue is uncertain. For this reason, each system was simulated both with Asp12 protonated and deprotonated. In the case of the native structure, only when Asp12 was deprotonated was the structure stable. For the native reduced and the intermediate, the protonation of Asp12 did not significantly affect the configurations sampled during the simulations.

ACCESSION NUMBERS

Coordinates for the structures of the MCoTI-II intermediate II_a have been deposited in the Protein Data Bank under ID code 2po8.

SUPPLEMENTAL DATA

Supplemental Data include one table and Supplemental References and can be found with this article online at http://www.structure.org/cgi/content/full/16/6/842/DC1/.

ACKNOWLEDGMENTS

The studies described herein were supported by grants from the Australian Research Council (ARC). M.C. is an ARC Postdoctoral Fellow, N.L.D. is a National Health and Medical Research Council Industry Fellow, D.J.C. is an ARC Professorial Fellow, and A.E.M. is an ARC Federation Fellow.

Received: April 26, 2007
Revised: January 16, 2008
Accepted: February 19, 2008
Published: June 10, 2008

REFERENCES

Anfinsen, C.B. (1973). Principles that govern the folding of protein chains. Science *181*, 223–230.

Arolas, J.L., D'Silva, L., Popowicz, G.M., Aviles, F.X., Holak, T.A., and Ventura, S. (2005a). NMR structural characterization and computational predictions of the major intermediate in oxidative folding of leech carboxypeptidase inhibitor. Structure *13*, 1193–1202.

Arolas, J.L., Popowicz, G.M., Bronsoms, S., Aviles, F.X., Huber, R., Holak, T.A., and Ventura, S. (2005b). Study of a major intermediate in the oxidative folding of leech carboxypeptidase inhibitor: contribution of the fourth disulfide bond. J. Mol. Biol. *352*, 961–975.

Arolas, J.L., Aviles, F.X., Chang, J.Y., and Ventura, S. (2006). Folding of small disulfide-rich proteins: clarifying the puzzle. Trends Biochem. Sci. *31*, 292–301.

Berendsen, H.J.C., Postma, J.P.M., Van Gunsteren, W.F., and Hermans, J. (1981). Interaction models for water in relation to protein hydration. In Intermolecular Forces, B. Pullman, ed. (Dordrecht: Reidel).

Berendsen, H.J.C., Postma, J.P.M., Van Gunsteren, W.F., DiNola, A., and Haak, J.R. (1984). Molecular dynamics with coupling to an external bath. J. Chem. Phys. *81*, 3684–3690.

Bonander, N., Leckner, J., Guo, H., Karlsson, B.G., and Sjolin, L. (2000). Crystal structure of the disulfide bond-deficient azurin mutant C3A/C26A: how important is the S-S bond for folding and stability? Eur. J. Biochem. *267*, 4511–4519.

Brünger, A.T., Adams, P.D., and Rice, L.M. (1997). New applications of simulated annealing in X-ray crystallography and solution NMR. Structure *5*, 325–336.

Cemazar, M., Zahariev, S., Lopez, J.J., Carugo, O., Jones, J.A., Hore, P.J., and Pongor, S. (2003). Oxidative folding intermediates with nonnative disulfide bridges between adjacent cysteine residues. Proc. Natl. Acad. Sci. USA *100*, 5754–5759.

Cemazar, M., Zahariev, S., Pongor, S., and Hore, P.J. (2004). Oxidative folding of Amaranthus α-amylase inhibitor: disulfide bond formation and conformational folding. J. Biol. Chem. *279*, 16697–16705.

Cemazar, M., Daly, N.L., Haggblad, S., Lo, K.P., Yulyaningsih, E., and Craik, D.J. (2006). Knots in rings. The circular knotted protein *Momordica cochinchinensis* trypsin inhibitor-II folds via a stable two-disulfide intermediate. J. Biol. Chem. *281*, 8224–8232.

Chiche, L., Heitz, A., Gelly, J.C., Gracy, J., Chau, P.T.T., Ha, P.T., Hernandez, J.F., and Le Nguyen, D. (2004). Squash inhibitors: from structural motif to macrocyclic knottins. Curr. Protein Pept. Sci. *5*, 341–349.

Colgrave, M.L., and Craik, D.J. (2004). Thermal, chemical, and enzymatic stability of the cyclotide kalata B1: the importance of the cyclic cystine knot. Biochemistry *43*, 5965–5975.

Craik, D.J. (2006). Chemistry. Seamless proteins tie up their loose ends. Science *311*, 1563–1564.

Craik, D.J., and Daly, N.L. (2005). Oxidative folding of the cystine knot motif in cyclotide proteins. Protein Pept. Lett. *12*, 147–152.

Craik, D.J., Daly, N.L., Bond, T., and Waine, C. (1999). Plant cyclotides: a unique family of cyclic and knotted proteins that defines the cyclic cystine knot structural motif. J. Mol. Biol. *294*, 1327–1336.

Craik, D.J., Daly, N.L., and Waine, C. (2001). The cystine knot motif in toxins and implications for drug design. Toxicon *39*, 43–60.

Craik, D.J., Daly, N.L., Mulvenna, J., Plan, M.R., and Trabi, M. (2004). Discovery, structure and biological activities of the cyclotides. Curr. Protein Pept. Sci. *5*, 297–315.

Craik, D.J., Cemazar, M., and Daly, N.L. (2006a). The cyclotides and related macrocyclic peptides as scaffolds in drug design. Curr. Opin. Drug Discov. Devel. *9*, 251–260.

Craik, D.J., Cemazar, M., Wang, C.K., and Daly, N.L. (2006b). The cyclotide family of circular miniproteins: nature's combinatorial peptide template. Biopolymers *84*, 250–266.

Creighton, T. (1974). Intermediates in the refolding of reduced pancreatic trypsin inhibitor. J. Mol. Biol. *87*, 579–602.

Daly, N.L., Clark, R.J., and Craik, D.J. (2003). Disulfide folding pathways of cystine knot proteins. Tying the knot within the circular backbone of the cyclotides. J. Biol. Chem. *278*, 6314–6322.

Felizmenio-Quimio, M.E., Daly, N.L., and Craik, D.J. (2001). Circular proteins in plants: solution structure of a novel macrocyclic trypsin inhibitor from *Momordica cochinchinensis*. J. Biol. Chem. *276*, 22875–22882.

Goransson, U., Svangard, E., Claeson, P., and Bohlin, L. (2004). Novel strategies for isolation and characterization of cyclotides: the discovery of bioactive macrocyclic plant polypeptides in the Violaceae. Curr. Protein Pept. Sci. *5*, 317–329.

Guntert, P., Mumenthaler, C., and Wüthrich, K. (1997). Torsion angle dynamics for NMR structure calculation with the new program DYANA. J. Mol. Biol. *273*, 283–298.

Gustafson, K.R., McKee, T.C., and Bokesch, H.R. (2004). Anti-HIV cyclotides. Curr. Protein Pept. Sci. *5*, 331–340.

Heitz, A., Chiche, L., Le-Nguyen, D., and Castro, B. (1995). Folding of the squash trypsin inhibitor EETI II. Evidence of native and non-native local structural preferences in a linear analogue. Eur. J. Biochem. *233*, 837–846.

Heitz, A., Hernandez, J.F., Gagnon, J., Hong, T.T., Pham, T.T., Nguyen, T.M., Le-Nguyen, D., and Chiche, L. (2001). Solution structure of the squash trypsin inhibitor MCoTI-II. A new family for cyclic knottins. Biochemistry *40*, 7973–7983.

Hernandez, J.F., Gagnon, J., Chiche, L., Nguyen, T.M., Andrieu, J.P., Heitz, A., Trinh Hong, T., Pham, T.T., and Le Nguyen, D. (2000). Squash trypsin inhibitors from *Momordica cochinchinensis* exhibit an atypical macrocyclic structure. Biochemistry *39*, 5722–5730.

Hutchinson, E.G., and Thornton, J.M. (1996). PROMOTIF—a program to identify and analyze structural motifs in proteins. Protein Sci. *5*, 212–220.

Laity, J.H., Lester, C.C., Shimotakahara, S., Zimmerman, D.E., Montelione, G.T., and Scheraga, H.A. (1997). Structural characterization of an analog of the major rate-determining disulfide folding intermediate of bovine pancreatic ribonuclease A. Biochemistry *36*, 12683–12699.

Laskowski, R.A., Rullmannn, J.A., MacArthur, M.W., Kaptein, R., and Thornton, J.M. (1996). AQUA and PROCHECK-NMR: programs for checking the quality of protein structures solved by NMR. J. Biomol. NMR *8*, 477–486.

Le-Nguyen, D., Heitz, A., Chiche, L., El Hajji, M., and Castro, B. (1993). Characterization and 2D NMR study of the stable [9-21, 15-27] 2 disulfide intermediate in the folding of the 3 disulfide trypsin inhibitor EETI II. Protein Sci. *2*, 165–174.

Linge, J.P., and Nilges, M. (1999). Influence of non-bonded parameters on the quality of NMR structures: a new force field for NMR structure calculation. J. Biomol. NMR *13*, 51–59.

Lovelace, E.S., Armishaw, C.J., Colgrave, M.L., Wahlstrom, M.E., Alewood, P.F., Daly, N.L., and Craik, D.J. (2006). Cyclic MrlA: a stable and potent cyclic conotoxin with a novel topological fold that targets the norepinephrine transporter. J. Med. Chem. *49*, 6561–6568.

Miller, J.A., Narhi, L.O., Hua, Q.X., Rosenfeld, R., Arakawa, T., Rohde, M., Prestrelski, S., Lauren, S., Stoney, K.S., and Tsai, L. (1993). Oxidative refolding of insulin-like growth factor 1 yields two products of similar thermodynamic stability: a bifurcating protein-folding pathway. Biochemistry *32*, 5203–5213.

Oostenbrink, C., Villa, A., Mark, A.E., and van Gunsteren, W.F. (2004). A biomolecular force field based on the free enthalpy of hydration and solvation: the GROMOS force-field parameter sets 53A5 and 53A6. J. Comput. Chem. *25*, 1656–1676.

Pallaghy, P.K., Nielsen, K.J., Craik, D.J., and Norton, R.S. (1994). A common structural motif incorporating a cystine knot and a triple-stranded β-sheet in toxic and inhibitory polypeptides. Protein Sci. *3*, 1833–1839.

Pearson, M.A., Karplus, P.A., Dodge, R.W., Laity, J.H., and Scheraga, H.A. (1998). Crystal structures of two mutants that have implications for the folding of bovine pancreatic ribonuclease A. Protein Sci. *7*, 1255–1258.

Rice, L.M., and Brünger, A.T. (1994). Torsion angle dynamics: reduced variable conformational sampling enhances crystallographic structure refinement. Proteins *19*, 277–290.

Rosengren, K.J., Daly, N.L., Plan, M.R., Waine, C., and Craik, D.J. (2003). Twists, knots, and rings in proteins. Structural definition of the cyclotide framework. J. Biol. Chem. *278*, 8606–8616.

Scheraga, H.A., Wedemeyer, W.J., and Welker, E. (2001). Bovine pancreatic ribonuclease A: oxidative and conformational folding studies. Methods Enzymol. *341*, 189–221.

Scott, W.R.P., Hunenberger, P.H., Tironi, I.G., Mark, A.E., Billeter, S.R., Fennen, J., Torda, A.E., Huber, T., and van Gunsteren, W.F. (1999). The GROMOS biomolecular simulation program package. J. Phys. Chem. A *103*, 3596–3607.

Shimotakahara, S., Rios, C.B., Laity, J.H., Zimmerman, D.E., Scheraga, H.A., and Montelione, G.T. (1997). NMR structural analysis of an analog of an intermediate formed in the rate-determining step of one pathway in the oxidative folding of bovine pancreatic ribonuclease A: automated analysis of ^{1}H, ^{13}C, and ^{15}N resonance assignments for wild-type and [C65S, C72S] mutant forms. Biochemistry *36*, 6915–6929.

Staley, J.P., and Kim, P.S. (1992). Complete folding of bovine pancreatic trypsin inhibitor with only a single disulfide bond. Proc. Natl. Acad. Sci. USA *89*, 1519–1523.

Stein, E.G., Rice, L.M., and Brünger, A.T. (1997). Torsion-angle molecular dynamics as a new efficient tool for NMR structure calculation. J. Magn. Reson. *124*, 154–164.

van den Berg, B., Chung, E.W., Robinson, C.V., and Dobson, C.M. (1999). Characterisation of the dominant oxidative folding intermediate of hen lysozyme. J. Mol. Biol. *290*, 781–796.

Wedemeyer, W.J., Welker, E., Narayan, M., and Scheraga, H.A. (2000). Disulfide bonds and protein folding. Biochemistry *39*, 4207–4216.

Weissman, J.S., and Kim, P.S. (1991). Reexamination of the folding of BPTI: predominance of native intermediates. Science *253*, 1386–1393.